ELSEVIER

Polymer 42 (2001) 305–317

polymer

www.elsevier.nl/locate/polymer

Morphology build-up in dendritic hyperbranched polymer modified epoxy resins: modelling and characterization

R. Mezzenga[1], C.J.G. Plummer, L. Boogh, J.-A.E. Månson*

Laboratoire de Technologie des Composites et Polymères (LTC), École Polytechnique Fédérale de Lausanne (EPFL), CH-1015 Lausanne, Switzerland

Received 10 November 1999; received in revised form 29 February 2000; accepted 6 April 2000

Abstract

The influence of cure temperature, composition and chemical structure on the morphology resulting from chemically induced phase separation has been investigated for different epoxy functionalized dendritic hyperbranched polymers blended with diglycydil bisphenol A and an aliphatic diamine. The cure temperature window chosen highlighted the influence of both the kinetics of phase separation and the thermodynamics of mixing on the final morphology. In relatively immiscible blends and at low cure temperatures, phase separation occurred immediately after mixing. However, increasing the miscibility by raising the temperature or modifying the chemistry of the dendritic hyperbranched polymers resulted in a homogeneous mixture prior to cure, and at low modifier contents, cure induced phase separation was thought to be associated with homogeneous nucleation of modifier rich spherical domains. Complete suppression of the phase separation could be achieved combining the effects of modifier solubility and reaction kinetics, by increasing the catalyst content in the most compatible blends.

Keywords: Dendritic hyperbranched polymers; Epoxy resins; Chemically induced phase separation

1. Introduction

Chemically induced phase separation (CIPS) is one of the number of techniques used to improve the fracture toughness of thermosets by promoting a two phase morphology [1,2]. In CIPS, the morphology develops during curing of an initially homogeneous mixture of the resin and a suitable modifier. This process depends on the several intrinsic and extrinsic parameters. The former relate mainly to the chemistry of the blend, whereas the latter, including pressure, temperature and composition, define the processing conditions.

The effect of cure temperature, T_c, on the morphology obtained by CIPS has been widely investigated for different types of linear modifier, leading to apparently conflicting results. The final volume fraction of the dispersed phase, V, as a function of T_c, for example, has been reported to show little change [3–5], a maximum at intermediate T_c [6] or a monotonic decrease with increasing T_c [7]. It will be argued here that any one of these trends might be anticipated for a given system, depending on the balance of kinetic and thermodynamic factors.

Varying the modifier content is another way of influencing the final morphology, as has been shown in rubber modified epoxy resins, for example [8–10]. V and the mean diameter of the dispersed phase domains, $\bar{D}$, have both been observed to increase with increasing modifier content, although total number of particles per unit volume, N_{tot}, tends to decrease. Adjusting the modifier content is also an effective way of inducing spinodal decomposition and obtaining co-continuous morphologies [11].

The influence of changes in the solubility of the modifier in the matrix has been investigated in acrylonitrile–butadiene random copolymer modified epoxy resins [12]. In order to modify the miscibility, the acrylonitrile/butadiene ratio may be varied, or different functional groups, such as carboxyls, epoxies and amines, can be grafted to the chain ends. However the effects of end-group functionalization on the morphology are limited, at least in the system in Ref. [12].

In what follows, the effect of varying the cure temperature, the blend composition and the modifier chemistry on the cure-induced phase separation in blends of a commercial epoxy-based thermoset and dendritic hyperbranched

* Corresponding author. Tel.: +41-21-693-4281; fax: +41-21-693-5880.
E-mail addresses: raffaele.mezzenga@epfl.ch (R. Mezzenga), jan-anders.manson@epfl.ch (J.-A.E. Månson).
[1] Tel.: +41-21-693-5995; fax: +41-21-693-5880.

0032-3861/01/$ - see front matter
PII: S0032-3861(00)00307-4

polymers (HBPs) is described. Such systems are currently of considerable interest owing to the relatively efficient toughening effect of HBPs [13]. CIPS provides great potential for controlling their morphology and hence optimizing their properties. It also has the advantage of limiting the influence of the reinforcing phase on the matrix morphology in composite materials. In an end-group functionalized three-generation HBP, such as those used in the present study, the number of reactive groups per molecule can be as high as 32. Thus, the chemistry and hence the solubility of the modifier are expected to play a more important role in HBPs than in end-group functionalized linear polymers. Moreover, since the HBP conformations are presumed to be globular, with the functional groups forming an external shell, shielding by the remainder of the molecule may be diminished with respect to that in a linear polymer. Finally, another potential means of influencing the final morphology investigated here was the catalyst content, which is expected to become a significant factor in morphological development as the cure rate becomes comparable with the rate of phase separation.

2. Experimental

The thermoset resin was diglycidyl ether bisphenol A (DGEBA) (Shell Epon 828), cured with isophorone diamine (IPD) (Fluka). Three different experimental grades of 3-generation epoxy functionalized HBPs, supplied by Perstorp, were used as modifiers. These differed in their epoxy equivalent weights (EEW) and hence in their solubility in the resin. They are referred to as HBP40, HBP60 and HBP95, having an EEW of 1050, 563 and 408 g/equivalent, respectively.

To investigate the effect of varying the composition, HBP pseudo-components, consisting of stochiometric mixtures of the HBP and the IPD, were blended with the resin in proportions ranging from 5 to 200 parts per hundred parts of resin (phr), corresponding to HBP concentrations of between 5 and 65% by volume. The term "resin" refers to a stochiometric mixture of DGEBA and IPD. To investigate the effect of varying T_c, use was made of a temperature gradient oven, allowing simultaneous cure over a range of T_c. This consisted of an 8 mm diameter glass tube containing the blend, inserted into an aluminum sleeve. The temperatures of the two ends of the oven were maintained at 21 and 160°C, respectively and 18 thermocouples placed along its length were used to monitor the temperature gradient, which was found to be linear to within experimental error. Rheological measurements were carried out using a Rheometrics RDA 2 analyzer at frequencies of 0.1, 1 and 10 Hz. To achieve the required torque sensitivity, parallel plates of 50 mm in diameter were used at an applied strain of 40%. The complex viscosity was recorded during dynamic temperature scans between 20 and 100°C at 20°C/min.

For quantitative morphological characterization, scanning electron micrographs of cryo-fractured surfaces were digitized, and analysed using the Optilab software package (Graftek). For cure conditions under which the particles became sufficiently large, the evolution of the morphology was monitored in situ by hot-stage optical microscopy of films of the blends placed between glass cover slides. Additional measurements were made by transmission electron microscopy (TEM) of thin sections of between 50 and 150 nm in thickness prepared from samples immersed overnight in a solution of RuO_4 using an ultramicrotome (Reichart-Jung Ultracut E) and a 35° diamond knife (Diatome). They were observed using the Philips EM 430 TEM at 300 kV.

Since the fracture surfaces were approximately planar, it was assumed that they intersected the particles at random. This assumption was later checked by comparison with the results from SEM of microtomed surfaces as will be discussed later. The particle size distribution was then determined from the diameters of the particles themselves, using a numerical procedure described elsewhere [14]. The results are given in terms of V, $\bar{D}$, N_{tot} and the maximum observed particle diameter, D_{max}. The distributions are expressed as the probability of the particle diameter's falling into one of n classes, each defined by a given sub-range of diameters. Thus the probability $p(i)$ that the particle diameter is in the ith class is

$$p(i) = \frac{N_v(i)}{\sum_{j=1}^{n} N_v(j)} \tag{1}$$

where $N_v(i)$ is the total number of particles with diameters in the ith class. The corresponding number average diameter is

$$\bar{D} = \sum_{j=1}^{n} p(j) D_j \tag{2}$$

where the D_j is the median of the diameter range defining the jth class. V was taken to be equal to the observed particle surface fraction, and N_{tot} was calculated from V using

$$V = N_{tot} \sum_{j=1}^{n} \left[\frac{4\pi p(j)}{3} \left(\frac{D_j}{2} \right)^3 \right] \tag{3}$$

At least 300 particle diameter measurements were used to determine $p(i)$ in any given sample.

3. Results and discussion

3.1. Morphological characterization

Fig. 1 shows the probability distribution of the average diameter, $\bar{D}$, determined from SEM of microtomed and fractured samples for a blend containing 10 phr of the HBP40-based pseudo-component cured at 80°C, whose post-cure morphology consisted of spherical HBP-rich domains in

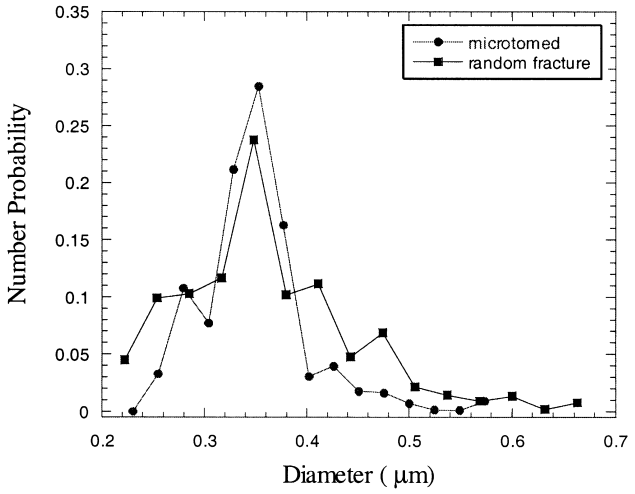

Fig. 1. Comparison of number probability distributions for the particle diameters obtained by SEM of fractured surfaces and microtomed surfaces.

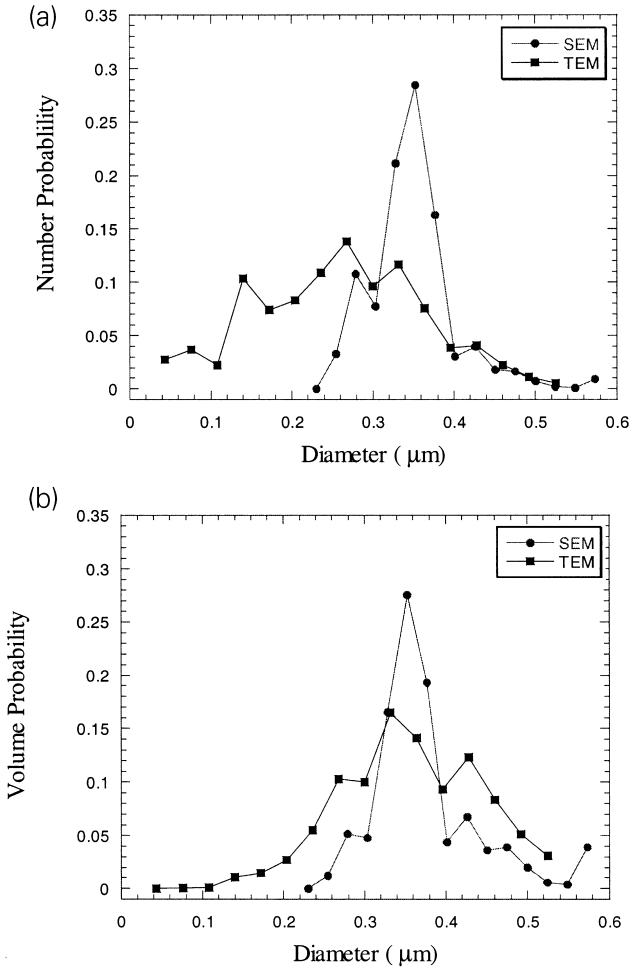

Fig. 2. Comparison of probability distributions for the particle diameters obtained by TEM and SEM: (a) number probability; and (b) volume probability.

an epoxy-rich matrix, indicating reasonable agreement between the results obtained using the two experimental methods. TEM analysis involved more lengthy sample preparation and was only used to verify the SEM results in a limited number of cases. In thin sections observed by TEM, one observes the projection either of whole particles or of sections through particles. Thus if the section is very much thicker than the diameter of the majority of the particles, their diameter distribution corresponds closely to the distribution of the observed diameters in the images. For larger particles, however, the diameters of the observed sections may be smaller than the original particle diameters. Nevertheless, by systematically varying the thickness of the sections, and assuming a homogeneous spatial distribution of the particle centres of mass, it is possible to estimate the diameter distributions and particle volume fractions in such cases, as described elsewhere [15].

Fig. 2a compares results from TEM and SEM for the same system as in Fig. 1. TEM clearly provided more information on the low diameter tail of the distributions than SEM, so that the calculated values of $\bar{D}$ were 0.260 μm from TEM as opposed to 0.348 μm from SEM. However the agreement appeared more reasonable if $p(i)$ was weighted by the particle volume and renormalized, as shown in Fig. 2b, leading to "volume average" particle diameters of 0.356 and 0.374 μm by TEM and SEM, respectively. Hence, although a large number of small particles were not detected by SEM, their contribution to the total volume of the second phase was relatively small. The limited resolution of the SEM method should nevertheless be borne in mind when considering the absolute values of $\bar{D}$ and N_{tot} referred to in what follows, all of which were determined from SEM micrographs.

3.2. The role of solubility

Decreasing the EEW, that is increasing the number of epoxy groups on the HBP shell at fixed total molecular weight, was anticipated to increase the initial solubility of the HBP in the epoxy resin. To gain an idea of the magnitude of this effect, solubility parameters have been estimated for a stiochiometric mixture of HBP and the amine, using the group contribution approach [16]. These are given in Table 1, along with estimated solubility parameters for DGEBA–IPD. The most soluble HBP is the one whose solubility parameters best

Table 1
Calculated solubility parameters for blends of the HBP–IPD/DGEBA–IPD pseudo-components

$(J/cm^3)^{1/2}$	HBP40	HBP60	HBP95	DGEBA
Dispersive	15.06	14.69	14.93	16.49
Polar	0.96	1.29	1.51	2.06
Hydrogen	7.95	8.13	8.20	7.44

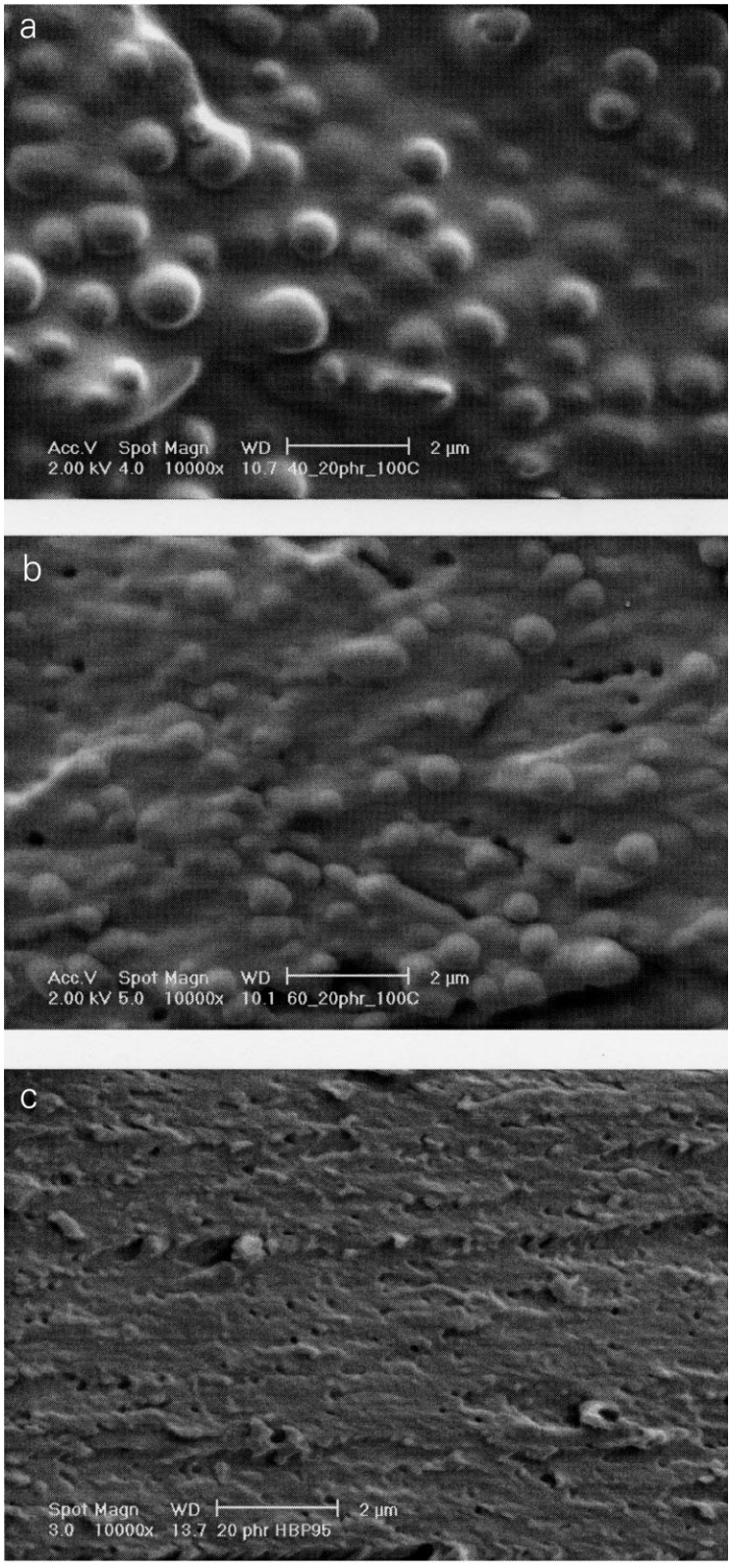

Fig. 3. Morphologies obtained by CIPS at 100°C in blends containing 20 phr of different HBP pseudo-components: (a) HBP40; (b) HBP60; and (c) HBP95.

match the ones of DGEBA. Thus, as expected, HBP95 is the most soluble in the resin, followed by HBP60 and HBP40, respectively.

Fig. 3 shows the morphology observed by SEM for 20 phr of the different HBP pseudo-components blended with the resin and cured at 100°C. Spherical second phase particles were again observed for HBP40, HBP60 and HBP95 suggesting phase separation to occur by nucleation and growth. Furthermore, the micrographs suggested a decrease in particle size as the miscibility between the resin and the modifier increased. Indeed, in the case of HBP95, the miscibility was sufficiently high to obtain such a fine structure, to remain almost visually transparent. The procedure of modifying final morphology by altering the modifier shell chemistry was shown to be unique to HBPs. In the specific class of HBPs used, the number of epoxy groups can be varied between 0 and 32, with an available range of functionalities sensibly larger than with other traditional modifiers.

These trends are shown more quantitatively in Fig. 4 using data from SEM micrographs. $\bar{D}$, D_{max} and V all decreased with decreasing EEW and hence with increasing solubility, while N_{tot} showed the opposite trend. Such dependence for N_{tot} was thought to be due to the significant particle coalescence at high initial nucleation densities, which would offset a trend towards greater nucleation densities with decreasing miscibility. Direct evidence for particle coalescence will be described in the next section.

The decrease in $\bar{D}$, D_{max} and V with increasing miscibility is thought to be linked both to the thermodynamics of mixing and the kinetics of demixing. Although the recent studies have shown that phase separation in blends of thermosets can continue within the dispersed domains well after the thermoset matrix gelation [17] (secondary phase separation), the conversion window available for primary phase separation is limited by the onset of phase separation and the gelation of the matrix. For a tetrafunctional amine–bifunctional epoxy, the theoretical gel point is at 58% conversion [18]. An experimental value of 60% was determined from the rheological measurements, assuming that the independence of tan(δ) upon the measurement frequency corresponds to the gel point [19]. The cloud point conversion versus blend composition was estimated using the Flory–Huggins approach, using evolving solubility parameters to calculate χ, as discussed in detail elsewhere [16,20]. Fig. 5 shows calculated phase diagrams for the three HBPs at 100°C showing the cloud point curves as a function of blend composition. In these graphs, concentrations are expressed in terms of the epoxy resin pseudo-component volume fraction. A significant shift of the cloud point to higher conversions as EEW is decreased at fixed T_c was predicted on this basis. It follows that: (i) the overall conversion window available for the phase separation and particle coalescence was reduced at low EEW; and (ii) that the matrix viscosity at the onset of phase separation increased as the cloud point conversion, and hence the degree of cross-linking, increased. Both the effects may be invoked to explain the observed decreases in $\bar{D}$, D_{max} and V.

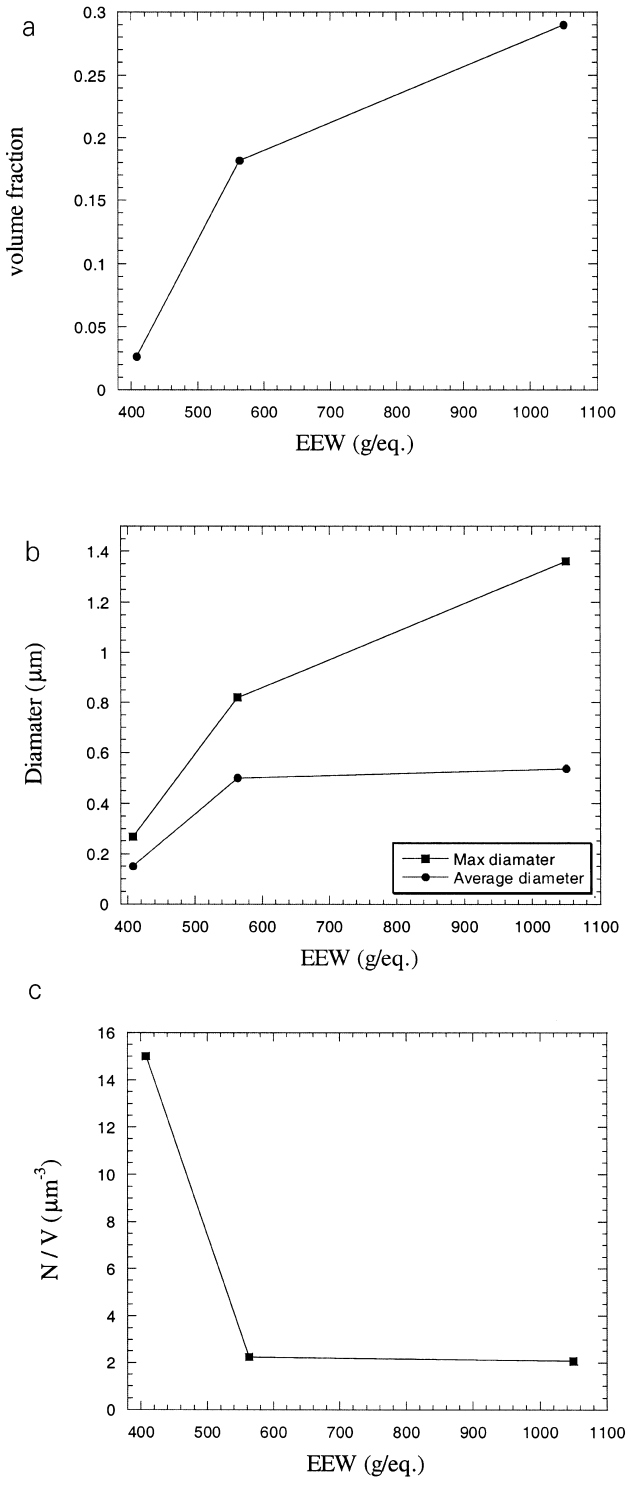

Fig. 4. Dependence of morphological parameters on EEW of the HBP: (a) volume fraction of the dispersed phase, V; (b) number average and maximum particle diameter, $\bar{D}$ and D_{max}; (c) number of particles per unit volume, N_{tot}.

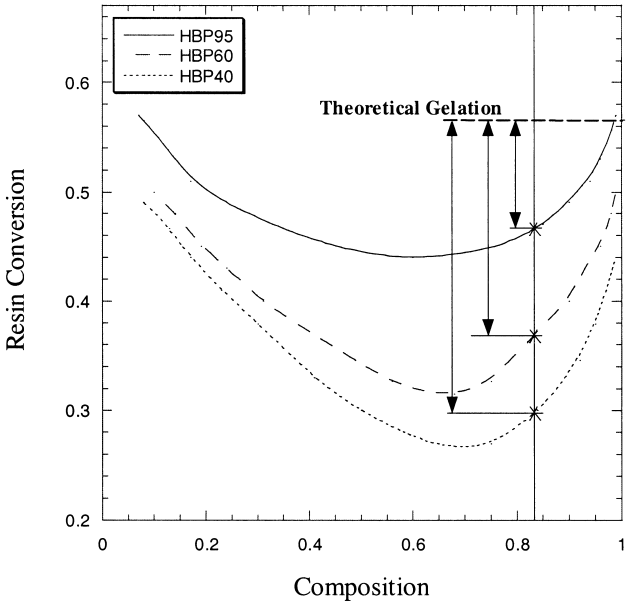

Fig. 5. Phase diagrams for the three epoxy resin-HBP blends showing the conversion at the cloud point as a function of the composition (compositions are expressed by volume fraction of the resin).

3.3. The role of curing temperature

As already mentioned, the cloud point is also moving to higher conversions for a given blend when the curing temperature, T_c is raised, since the value of χ estimated from the solubility parameters decreases as $1/T$. Although it is again possible to estimate the evolution of the conversion window in which phase separation is likely to occur, the evolution of morphology will also depend on how the phase separation kinetics is affected by T_c. Assuming homogeneous nucleation, the nucleation rate is:

$$\frac{dN}{dt} = N_o D \exp(-\Delta G_c/kT) \tag{4}$$

where N_o is a constant; D, the diffusion constant of modifier in the matrix; and ΔG_c is an activation energy. The growth rate of the dispersed phase is frequently described by:

$$r\frac{dr}{dt} = D(\phi_r - \phi_e) \tag{5}$$

where r is the particle radius and $\phi_r - \phi_e$ is the difference between the instantaneous concentration of the dispersed phase and its value at equilibrium [20]. D is assumed to be inversely proportional to the viscosity of the resin, η, as predicted, for example, by the Einstein relationship:

$$D = \frac{kT}{6\pi R_g \eta} \tag{6}$$

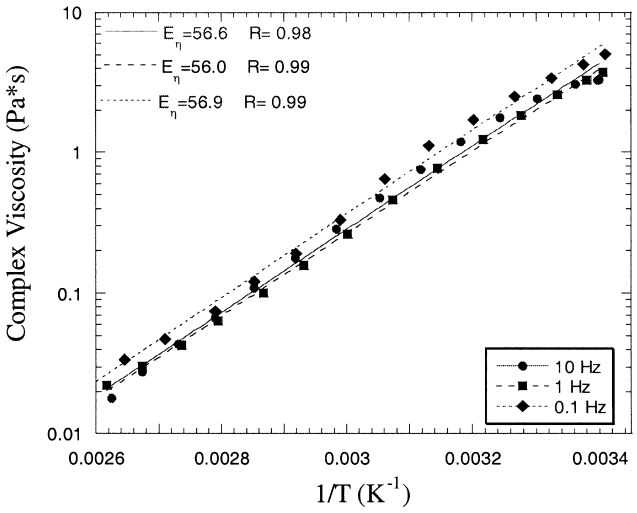

Fig. 6. Complex viscosity of the pure resin at zero conversion as measured using a parallel plate rheometer at 0.1, 1 and 10 Hz. R indicates the coefficient of correlation.

where R_g is the radius of gyration of the modifier and

$$\eta = A \exp\left(\frac{+E_A}{RT}\right) \tag{7}$$

where A is a front factor and E_A is the activation energy. Eq. (7) is consistent with the observed variation of η with temperature for uncured DGEBA/IPD, shown in Fig. 6, and it is inferred from Eqs. (4) to (7) that both the nucleation and growth rates should also show an exponential dependence on temperature for a given degree of conversion.

In Fig. 7, V has been given as a function of T_c for blends containing 10 and 20 phr of the HBP40, and 10 phr of the HBP60 pseudo-components. In both of the blends containing HBP40, V passed through a minimum, followed by a

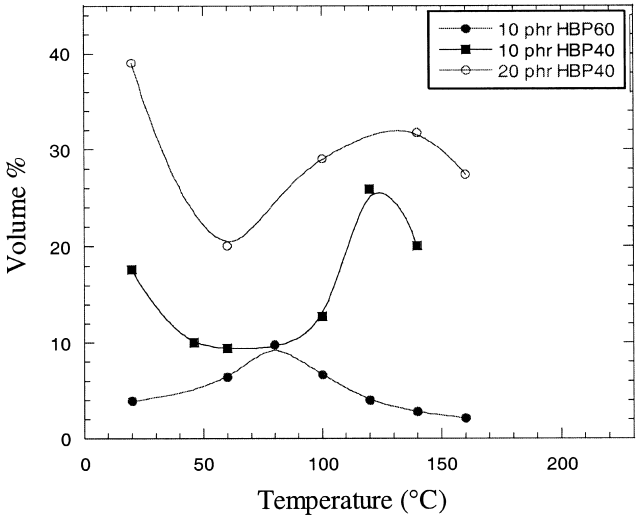

Fig. 7. V as a function of T_c for 10 and 20 phr of the HBP40 and 10 phr of the HBP60 pseudo-components.

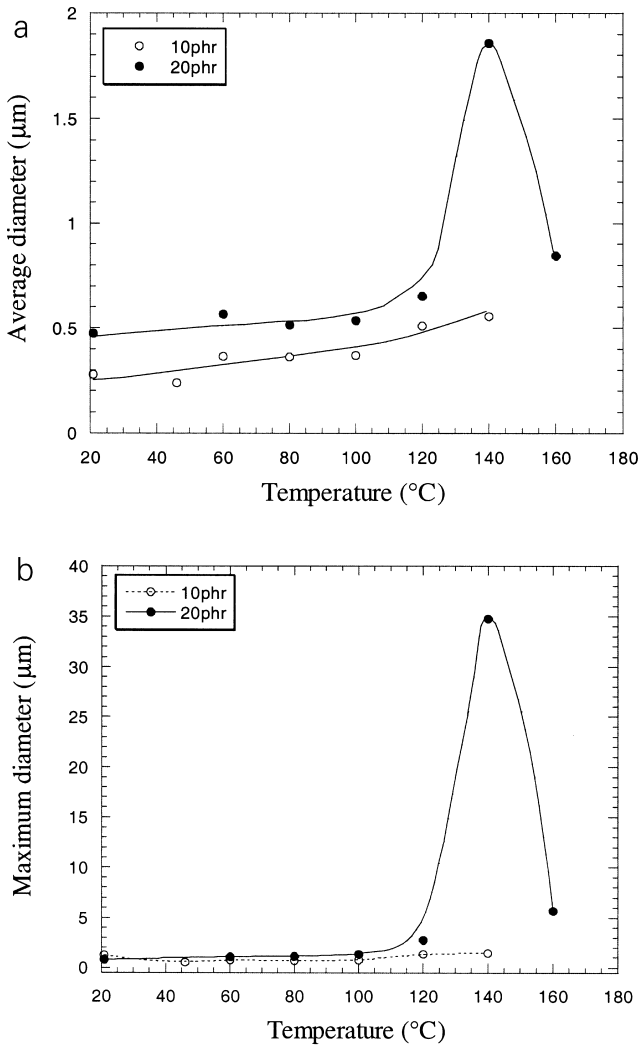

Fig. 8. (a) $\bar{D}$; and (b) D_{max} as a function of T_c for 10 and 20 phr of the HBP40 pseudo-component.

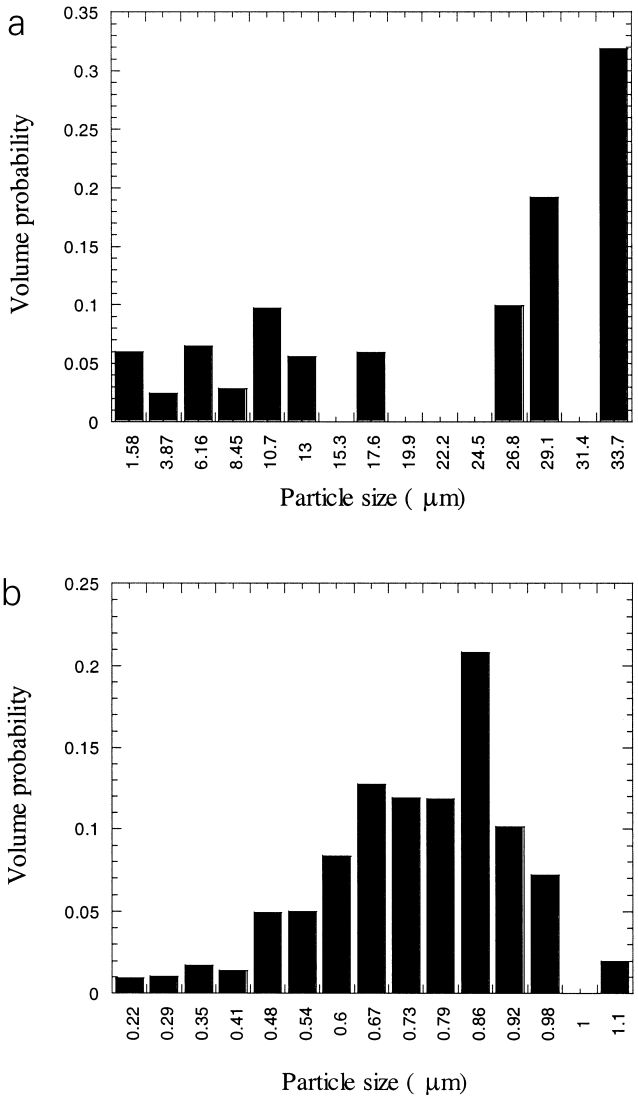

Fig. 9. Volume probability distribution of particle size expressed as a function of the average particle size of each class, for 20 phr of the HBP40 pseudo-component cured at different temperatures: (a) T_c = 140°C; and (b) T_c = 80°C.

maximum as T_c was increased from 20 to 160°C. The behaviour may be explained as follows. At 20°C, these blends spontaneously phase-separated after mixing and degassing, so that there was presumably no nucleation barrier to further phase separation during the subsequent cure. However, at somewhat higher T_c, they were initially fully miscible. Hence phase separation involved a nucleation step, and this was assumed to account for the observed decrease in the separated volume, V.

With further increase in T_c, the accompanying exponential increases in the nucleation and growth rates anticipated from Eqs. (4) to (7) were assumed to become dominant, leading to an increase in V, in spite of the increase in the cloud point conversion. Nevertheless, at the highest T_c, as the cloud point conversion approached the gel point, the narrowing of the conversion window for the phase separation and the increase in viscosity at the onset of phase separation may again be invoked to explain the observed decrease in V with T_c in this regime. It is significant in this respect that the maximum in $V(T_c)$ for 10 phr of the HBP40 pseudo-component occurred at a lower T_c than for 20 phr. This may be attributed to a higher cloud point conversion at a given T_c for the lower modifier content (cf. Fig. 4). Similar behaviour was observed for 10 phr of the HBP60 pseudo-component, with the exception of the minimum in $V(T_c)$, whose absence was assumed to be due to the miscibility of this blend at room temperature, HBP60 being more soluble in DGEBA/IPD than HBP40. This increase in miscibility also accounted for the shift of the maximum in $V(T_c)$ to a lower T_c than that for 10 phr of the HBP40 pseudo-component.

In Fig. 8a and b, $\bar{D}$ and D_{max} are shown for 10 and 20 phr of the HBP40 pseudo-component. For highly dispersed morphologies, the D_{max} becomes very large, as can be

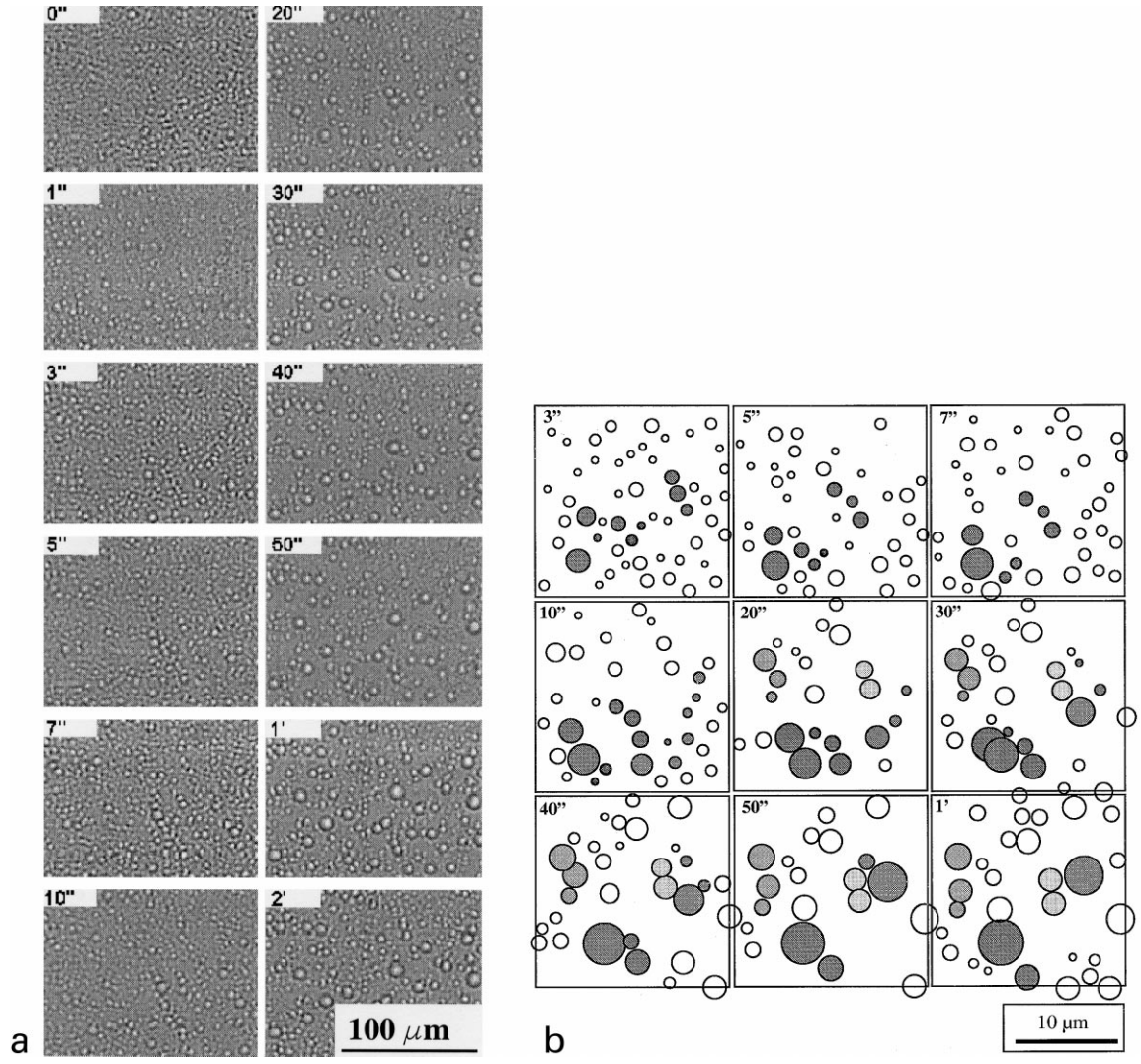

Fig. 10. (a) Time evolution of the morphology observed by optical microscopy for 20 phr of the HBP40 pseudo-component and $T_c = 140$°C over a period of 2 min ($t = 0$ corresponds to the cloud point). (b) Detail of (a) redrawn to illustrate particle coalescence (of the shaded particles for example).

seen from the scale of Fig. 8b. For both compositions, there was a slow monotonic increase in both quantities with T_c up to about 120°C. However, a much more abrupt increase was observed for 20 phr between 120 and 140°C. Moreover, the size distribution was markedly bimodal at 140°C, whereas those at lower T_c were monomodal, as illustrated in Fig. 9, where volume weighted probability distributions for 20 phr of HBP40 at 140 and 80°C are compared. These changes were associated with the optical observations of extensive particle coalescence in thin films of the same blend cured at 140°C. Fig. 10a shows a sequence of video captures for which $t = 0$ corresponds roughly to the cloud point. Individual second phase domains cannot be distinguished in the first frame, but there is a clear coarsening of the microstructure in subsequent frames. Fig. 10b is derived from a detail from the same sequence, in which clearly resolved particles have been represented by circles, and in which the shaded particles coalesced with each other during the reaction. It is significant that the extent of coalescence was not uniform within the films, but was associated with regions in which there was substantial capillary flow and/or convection. Large particles were therefore not seen in quiescent regions. This was consistent with the microstructure of bulk samples taken from the thermal gradient oven, in which the spatial distribution of particles of a given size was highly inhomogeneous. Indeed the trajectories of the larger particles could be identified from their "wakes", which were depleted of smaller particles.

It thus appears that massive particle coalescence, which occurred only for the higher concentration of the less soluble HBP, requires both a low η i.e. at a relatively low cloud point conversion and a high T_c, and a relatively high second phase content. It is also possible that coalescence was impeded in the later stages of the reaction by stabilization of the second phase, owing either to gelation or to

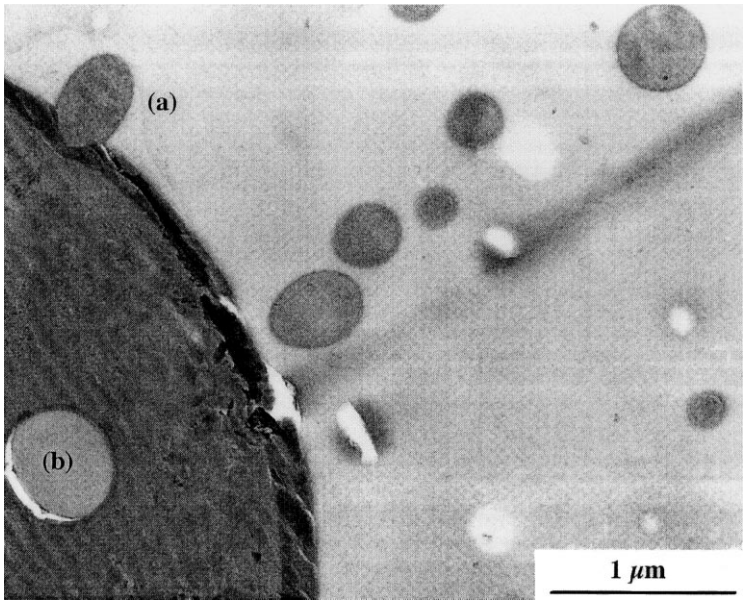

Fig. 11. TEM micrograph of particles in a sample containing 20 phr of the HBP40 pseudo-component and cured at $T_c = 140°C$ (ultrathin section of a sample stained by immersion in aqueous RuO_4): (a) distortion of the interface of a large modifier-rich particle in close proximity to a smaller particle; and (b) resin-rich inclusion in the large particle (the dark fringe around the large particle is due to over-staining of the resin and should be considered to form part of the matrix).

segregation of the most highly grafted HBP molecules, which had reacted the most with the resin, to the particle–matrix interfaces. This was inferred from the observation of considerable movement of the particles in the thin films at conversions beyond that at which coalescence apparently ceased. Indeed in TEM micrographs such as that in Fig. 11, particles in close proximity were separated by a thin layer of epoxy, with some local distortion of the interfaces which may be indicative of a relatively low interfacial tension. The figure also shows a recurrent feature of these samples, namely phase inversion, with one or two small epoxy rich inclusions being observed in the interior of the larger second phase particles.

3.4. The role of composition

The effect of composition on the blend morphology was investigated at 80°C using HBP60 as modifier which respectively correspond to average conditions of curing temperature and modifier solubility. In Fig. 12, V, $\bar{D}$, D_{max} and N_{tot} are shown as a function of the HBP pseudo-component content, and the morphologies are given in Fig. 13. Although the particle diameters and V increased with HBP content, N_{tot} decreased. The observation of essentially spherical particles for pseudo-component contents of up to 50 phr suggested nucleation and growth. This is consistent with Fig. 14, which shows the calculated phase diagram for HBP60/DGEBA/IPD at 80°C, for which the critical point corresponds to an HBP content of just over 50 phr. As shown in Fig. 13, an interpenetrated morphology was obtained at 100 phr, where the volume fractions of the modifier and the resin were approximately equal. At 200 phr, however, corresponding to 65% HBP by volume, the modifier was the continuous phase.

The morphologies obtained for HBP pseudo-component contents of up to 50 phr may be explained quantitatively in terms of the evolution of η with cloud point conversion as previously. The evolution of the particle size was also found to be consistent with previous observations of CIPS in modified epoxy resins. At low HBP contents it may be assumed that η was close to that of unmodified DGEBA/IPD. Since T_c was also constant, η was taken to be a function of conversion only. It has been argued by Verchère et al. on an empirical basis, that $\bar{D}$, in rubber modified epoxies, should be proportional to $\log(\eta_{CP})$, where η_{CP} is the viscosity at the cloud point [3]. There are a number of models for the evolution of η as a function of conversion and temperature, and in general, a complex dependence on the degree of conversion is anticipated, even under isothermal conditions [21–24]. Nevertheless, given the limited ranges of conversion in which phase separation occurred in the present case, η may be expressed by a simple exponential expression:

$$\eta(p) = B_1 \exp(-B_2(p_{GEL} - p)) \tag{8}$$

where p is the conversion; B_1 and B_2, the empirical constants; and p_{GEL}, the conversion at the gel point. Fig. 15 shows a fit of Eq. (8) to experimental data for η in DGEBA/IPD as a function of conversion, showing excellent agreement for conversions within the phase separation window. Thus, one can expect, from the observations of Verchère et al. on rubber modified epoxies, that $\bar{D}$ should be a linear function

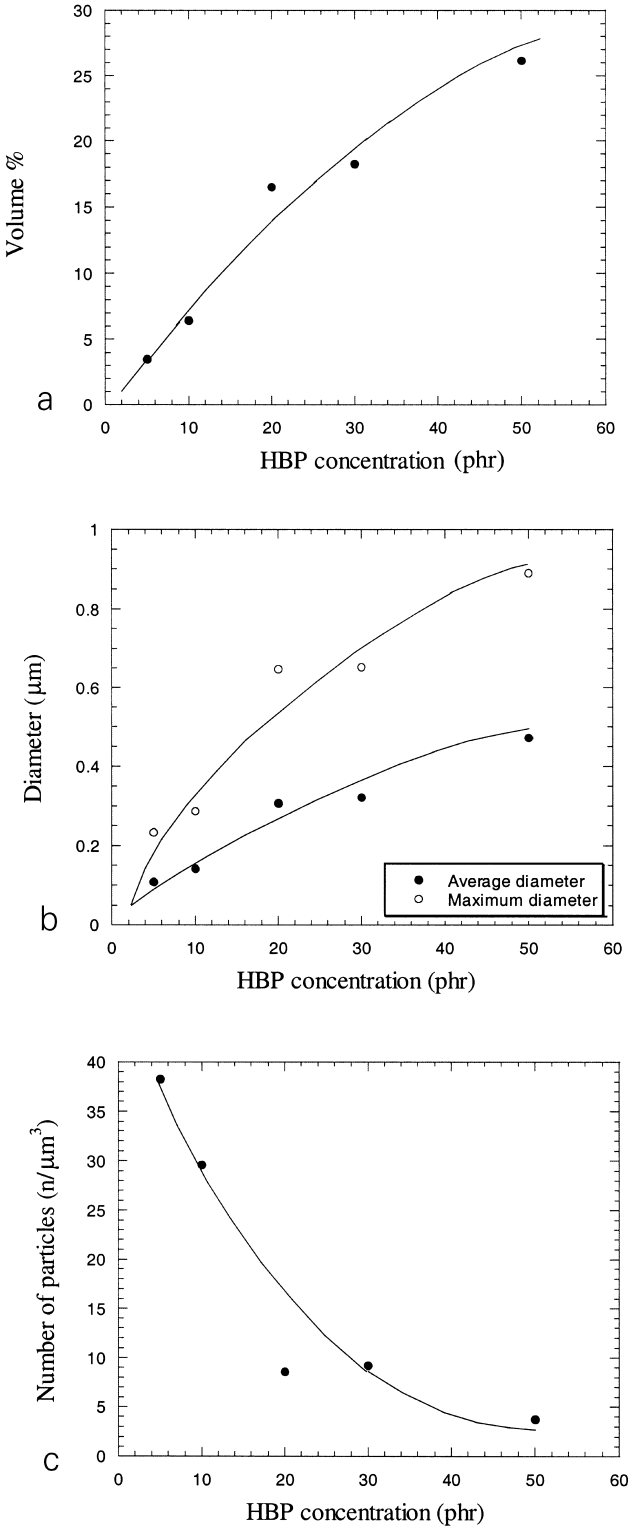

Fig. 12. Dependence of morphological parameters on composition for HBP60 and $T_c = 80°C$: (a) V; (b) $\bar{D}$ and D_{max}; and (c) N_{tot}.

of the cloud point conversion, p_{CP}. This is borne out by Fig. 16, in which the average particle diameter has been plotted against $p_{GEL} - p_{CP}$. Also shown in Fig. 16 is V, whose dependence on p_{CP} was also close to linear.

3.5. The role of catalyst content

Catalysts are normally added to thermosets in very low concentrations, and therefore the overall composition and miscibility of the blend are not affected significantly. However, the presence of a catalyst increases the cure rate, so that the morphology may depend on the extent to which the phase separation rate can keep up with the cure rate. For phase separation by nucleation and growth, the evolution of characteristic quantities such as $\bar{D}$ and V, may be anticipated broadly to follow the ratio between the "phase separation rate" K_{PS} and polymerization rate K_{PR} [11].

Although the phase separation rate is not explicitly defined here, it is assumed to be proportional to the diffusion constant and independent of the catalyst concentration. In Fig. 17, $\bar{D}$ and V are plotted for T_c of 60 and 120°C, for 10 phr of the HBP40 pseudo-component. When the catalyst concentration was increased at constant T_c, $\bar{D}$ decreased, and when the catalyst concentration was sufficiently high, phase separation was suppressed altogether. Fig. 17 also gives an indication of the effect of T_c. The catalyst concentration at which the transition between the heterogeneous and homogeneous final microstructures occurred decreased with T_c, at high T_c the morphology appearing more sensitive to the catalyst concentration. This may again be explained by a shift in the cloud point towards higher conversions with increasing T_c.

4. Conclusions

The effect of dendritic hyperbranched polymers shell chemistry, cure temperature, and composition on the morphology of HBP/DGEBA/IPD blends has been characterized in terms of the size of the second phase domains, their number per unit volume and their total volume fraction V, all characterized by electron and optical microscopy.

Increasing the number of epoxy groups onto the HBP shell, i.e. decreasing their EEW, resulted in an increased miscibility of the modifier into the epoxy resin. This could be predicted by the shift of theoretical phase diagrams with the number of epoxy groups onto the HBP shell. The experimental evidence of this compatibilization was the refining of the final morphology coarseness observed by comparing the effect of the least, medium and most compatible modifiers.

An observed increase in the particle size and V with T_c for a given system was attributed to the decrease in η with T_c, which was assumed to facilitate nucleation and growth. Coalescence between particles was also observed to be an important factor, at least for the least soluble modifier cured at 140°C, for which a markedly bimodal particle size distribution was observed. However, in order to explain the

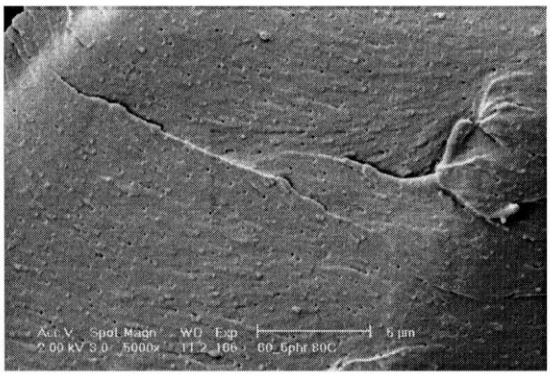

5 phr

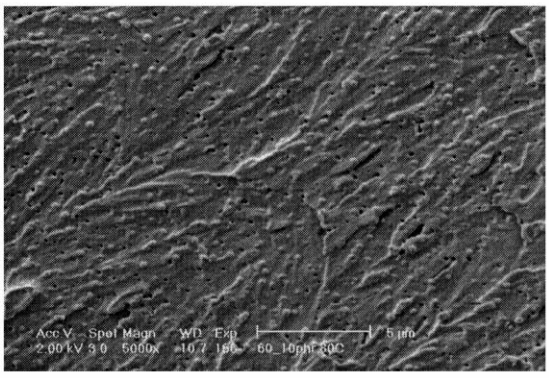

10 phr

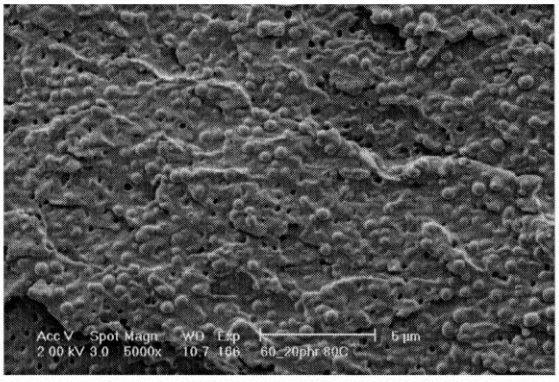

20 phr

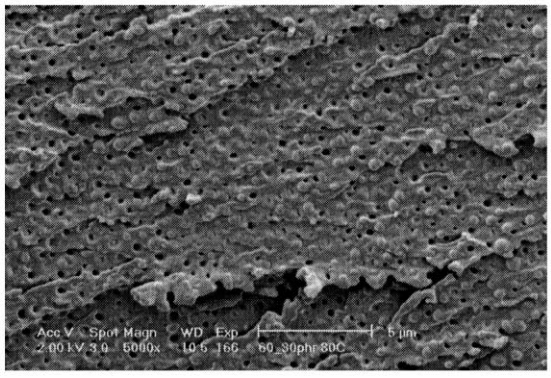

30 phr

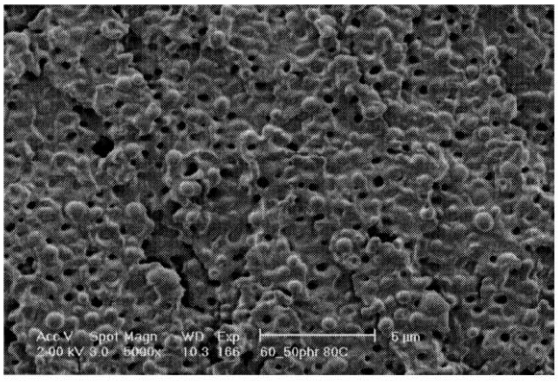

50 phr

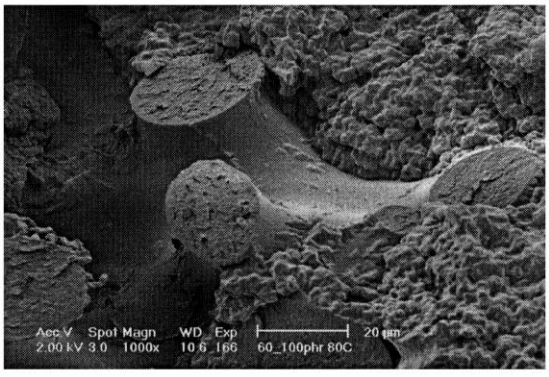

100 phr

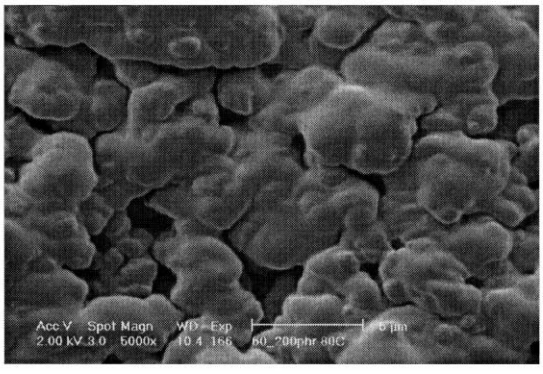

200 phr

Fig. 13. SEM micrographs of fracture surfaces for HBP60 and $T_c = 80°C$, and compositions between 5 and 200 phr of the pseudo-component (5–65% by volume).

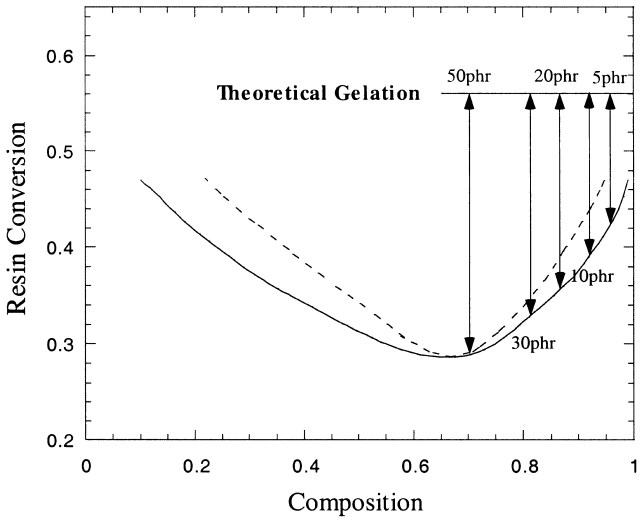

Fig. 14. Phase diagram for HBP60 and $T_c = 80°C$ showing the conversion at the cloud point as a function of the composition (compositions are expressed as volume fractions of the resin).

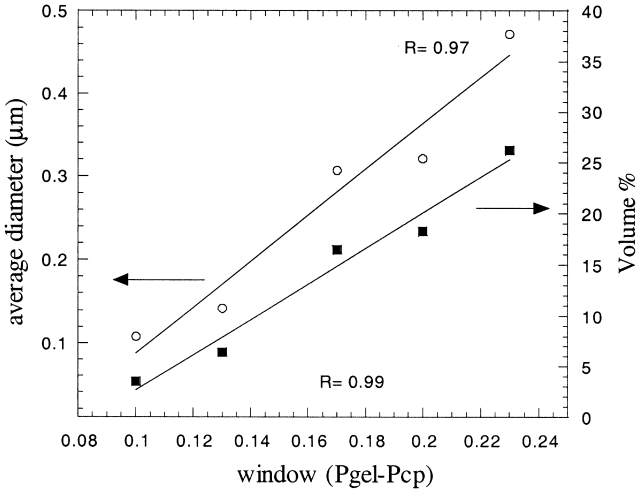

Fig. 16. Dependence of morphological parameters V; and $\bar{D}$ on the width of the conversion window corresponding to phase separation for 10 phr of the HBP40 pseudo-component.

trends over the full range of miscibility and T_c, it was also necessary to consider the evolution of the conversion corresponding to the cloud point. Indeed, for the most miscible blends, where the cloud point conversion approached the gel point, a really fine structure was observed. On the other hand, relatively coarse morphologies obtained at low T_c in the least miscible blends were associated with phase separation at zero conversion, so that there was no nucleation barrier to further phase separation. The tendency towards finer microstructures and lower second phase contents at intermediate T_c with increasing miscibility has been attributed both to an increase in the viscosity at the cloud point and to a narrowing of the conversion window for phase separation.

The variation of the blend morphology with HBP

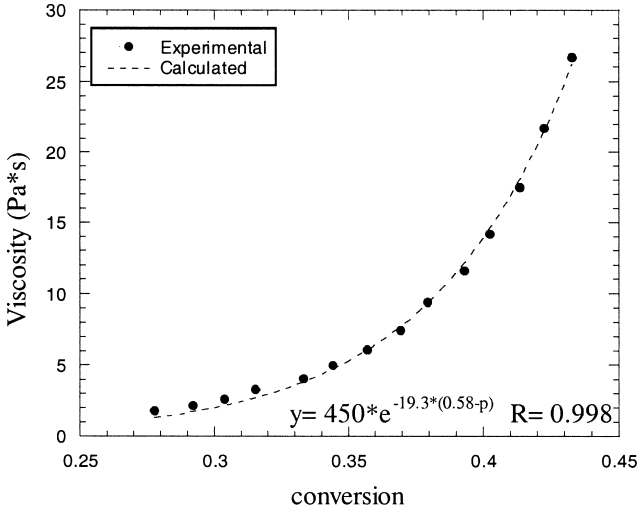

Fig. 15. Exponential fit to data for the complex viscosity of the unmodified resin in the phase separation region.

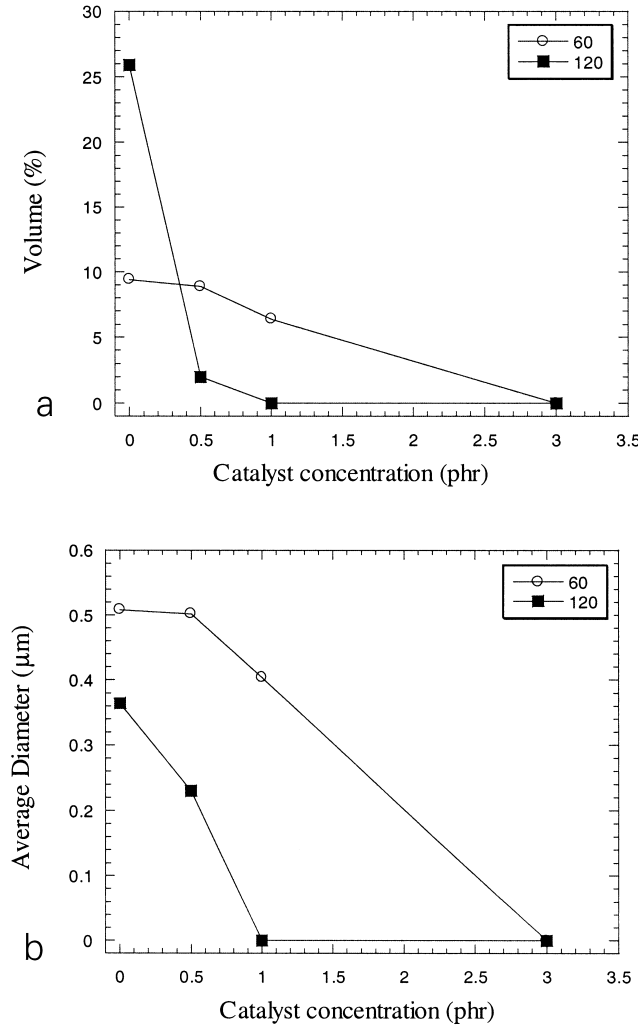

Fig. 17. Dependence of morphological parameters on catalyst concentration for $T_c = 60$ and 120°C for 10 phr of the HBP40 pseudo-component: (a) V; and (b) $\bar{D}$.

pseudo-component concentration in the range 0–50 phr was consistent with the previous results in the literature for thermoplastic and rubber modified epoxy systems. In particular, at any given T_c, the phase diagrams could be used to predict η at the cloud point, as a function of modifier concentration, by assuming it to show the same approximately exponential dependence on the degree of polymerization at low modifier contents as observed in the unmodified resin. The observed final particle sizes were found to be consistent with the empirical law proposed by Sautereau et al. according to which the mean particle diameter should show a logarithmic dependence on the viscosity at the cloud point. Further increasing the HBP content led first to co-continuous microstructures believed to be associated with spinodal decomposition, and at sufficiently high HBP contents, a microstructure consisting of epoxy rich domains in a continuous HBP rich matrix.

The effect of catalyst was also investigated for one of the systems of interest here. The increase in the cure rate of the epoxy with catalyst content was shown to be sufficient not only to diminish V and the particle size, but also to suppress the phase separation once the phase separation kinetics were no longer able to keep up with the cure rate. The microstructures were particularly sensitive to the catalyst content at high T_c, where the cloud point conversion was already relatively high.

Acknowledgements

Perstorp Specialty Chemicals is acknowledged for their financial support. Mr Bo Pettersson, from Perstorp, is also gratefully acknowledged for his contribution to fruitful discussions.

References

[1] Hedrick JL, Yilgor I, Jurek M, Hedrick JC, Wilkes GL, McGrath JE. Polymer 1991;32:2020.
[2] Hwang JF, Manson JA, Hertzberg RW, Miller GA, Sperling LH. Polym Engng Sci 1989;29:1466.
[3] Verchere D, Sautereau H, Pascault JP, Moschiar SM, Riccardi CC, Williams JJ. J Appl Polym Sci 1991;42:701.
[4] Butta E, Levita G, Marchetti A, Lazzeri A. Polym Engng Sci 1986;26:63.
[5] Chan LC, Gillham JK, Kinloch AJ, Shaw SJ. Rubber-modified thermoset resins. In: Riew CK, Kinloch AJ, editors. Washington, DC: Americal Chemical Society, 1984.
[6] Manzione LT, Gillham JK, McPherson CA. J Appl Polym Sci 1981;26:889.
[7] Manzione LT, Gillham JK, McPherson CA. J Appl Polym Sci 1981;26:907.
[8] Yamanaka K, Inoue T. J Mater Sci 1990;25:241.
[9] Kunz SC, Sayre JA, Assink RA. Polymer 1982;23:1897.
[10] Yamanaka K, Takagi Y, Inoue T. Polymer 1989;60:1839.
[11] Girard-Reyedet E, Sautereau H, Pascault JP, Keates P, Navard P, Thollet G, Vigier G. Polymer 1998;39:2269.
[12] Chen D, Pascault JP, Bertsch RJ, Drake RS, Siebert AR. J Appl Polym Sci 1994;51:1959.
[13] Boogh L, Pettersson B, Månson JAE. Polymer 1999;40:2249.
[14] Saltykov SA. Stereometric metallography. Moscow: Metallurgizdat, 1958.
[15] Plummer CJG, Hedrick JL, Hilborn JG. Polymer 1995;36:2485.
[16] Mezzenga R, Boogh L, Månson JAE. Submitted for publication.
[17] Riccardi CC, Borrajo J, Williams JJ. Polymer 1994;35:5541.
[18] Flory PJ. Principles of polymer chemistry. Ithaca, NY: Cornell University Press, 1953.
[19] Winter HH, Chambon F. J Rheol 1986;30:367.
[20] Vasquez A, Rojas AJ, Adabbo HE, Borrajo J, Williams JJ. Polymer 1987;28:1156.
[21] Mijovic J, Lee CH. J Appl Polym Sci 1989;38:2155.
[22] Kenny JM, Apicella A, Nicolais L. Polym Engng Sci 1989;29:973.
[23] Gillham JK, Enns JB. J Appl Polym Sci 1983;28:2567.
[24] Kenny JM, Maffezzoli A, Nicolais L. Compos Sci Technol 1990;38:339.